PERFORMANCE CHARACTERIZATION OF PNEUMATIC SINGLE PELLET INJECTION SYSTEM*

D. D. Schuresko, S. L. Milora, J. T. Hogan
C. A. Foster, and S. K. Combs

Oak Ridge National Laboratory
Oak Ridge, Tennessee 37830

ABSTRACT

The Oak Ridge National Laboratory single-shot pellet injector, which has been used in plasma fueling experiments on ISX and PDX, has been upgraded and extensively instrumented in order to study the gas dynamics of pneumatic pellet injection. An improved pellet transport line was developed which utilizes a 0.3-cm-diam by 100-cm-long guide tube. Pellet gun performance was characterized by measurements of breech and muzzle dynamic pressures and by pellet velocity and mass determinations. Velocities up to 1.4 km/s were achieved for intact hydrogen pellets using hydrogen propellant at 5-MPa breech pressure. These data have been compared with new pellet acceleration calculations which include the effects of propellant friction, heat transfer, time-dependent boundary conditions, and finite gun geometry. These results provide a basis for the extrapolation of present-day pneumatic injection system performance to velocities in excess of 2 km/s.

*Research sponsored by the Office of Fusion Energy, U.S. Department of Energy, under contract W-7405-eng-26 with the Union Carbide Corporation.

I. INTRODUCTION

Injection of high velocity hydrogen pellets is the lead tecnnology for fueling existent and future plasma fusion devices.[1] Central fueling of 1-keV plasmas has been achieved on ISX,[2] PDX,[3] and ASDEX[4] using $\lesssim$1-km/s pellets accelerated pneumatically by high pressure helium or hydrogen propellants. To meet the fueling requirements of the fusion feasibility demonstration experiments and future fusion power reactors, multiple injection of nominal 2-4-mm pellets at velocities in excess of 2 km/s will be required.[1]

The performance of the 0-1 km/s pneumatic injectors has been modelled with partial success by using the theory of a one-dimensional, centered rarefaction wave in an unbounded tube to calculate the force exerted by the propellant on a frictionless pellet.[5,6] The ideal gun theory neglects potentially important effects such as propellant friction, heat exchange, and finite gun geometry. A newly developed gas dynamic model which incorporates these effects has been tested by upgrading the Oak Ridge National Laboratory (ORNL) single pellet injector[5] with improved propellant and pellet diagnostics and extending the operational range of the device with helium and hydrogen propellants to temperatures as high as 400 K and pressures up to 5 MPa. Velocity scans under these conditions have been performed in the range of 0.4 to 1.4 km/s. The velocities achieved with helium propellant are within 20 percent of the ideal gun theory predictions; velocities obtained with hydrogen propellant, which are significantly less than ideal gun theory predictions, are adequately modelled by the more detailed gas dynamic treatment.

This theory, having been experimentally benchmarked against these data, now serves as a basis for the design of high velocity pneumatic injection systems.

II. EXPERIMENTAL DETAILS AND RESULTS

The single-shot pellet injector, which was developed by Milora and Foster,[5] has been modified for 1.6-mm-diam by 1.75-mm-long cylindrical pellets while retaining the original 16-cm-long barrel. Additional modifications were made to provide propellant pressure and temperature measurements. A piezoelectric pressure transducer* mounted at the outlet of the fast solenoid valve measures the gun breech pressure. A 25-W cartridge heater mounted in the valve body provides propellant heating; the propellant is warmed to the valve body temperature, which is measured by a chromel-alumel thermocouple. Gun muzzle pressures are measured with a second piezoelectric pressure transducer† mounted in a collar which captures the gun barrel for proper alignment.

The original pellet line (Fig. 5 of Ref. 5) has been equipped with a guide tube, a 0.3-cm-ID by 100-cm-long quartz tube inserted through the gas baffles (Fig. 1). Photodiodes located at both ends of this primary guide tube provide timing pulses for velocity measurements. Pellet shadowgraphs were obtained at the guide tube exit using a spark lamp triggered by a velocity compensating timing circuit.[7] Pellet impacts were measured with a shock accelerometer‡ mounted in an aluminum target, which was located at the outlet of the guide tube system. The shadowgraphs and the integrated impact shock signals were used to confirm pellet integrity and mass.

---

*PCB Piezotronics, Inc., Model 105B12.

†Entran Devices Model EPJ-070-500A.

‡PCB Piezotronics, Inc., Model 305A03.

Breech and muzzle pressure transients and the shadowgraph obtained for a typical 1-km/s helium-propelled pellet are shown in Fig. 2. In the top trace of Fig. 2(a), the chamber pressure rises to its maximum of 2.34 MPa in ∿0.3 ms. As a result of the finite volume in the valve body and the gun chamber, the breech pressure rises to only about two-thirds of the valve fill pressure. The subsequent decay of the pressure is caused by an increase in the system volume as the pellet moves through the gun barrel.* The timing pulse generated by photodiode PD1 of Fig. 1, which marks the exit of the pellet from the gun muzzle pressure transducer collar, is displayed in the bottom trace of Fig. 2(a). The muzzle pressure, displayed in the center trace of Fig. 2(a), rises abruptly to approximately 0.10 MPa when the pellet exits the gun barrel and continues to rise to 0.14 MPa before tailing off. The pellet itself is shown in Fig. 2(b). The pellet has tumbled during its post acceleration passage through the guide tube but still conforms very well to its original 1.6-mm-diam by 1.75-mm-long dimensions.

Pellet velocities obtained for room temperature helium gas and heated helium and hydrogen propellants at pressures ranging from 1 to 5 MPa are plotted in Fig. 3. The abscissa in this figure, L/τ, is the gun barrel length L divided by the characteristic pellet acceleration time τ of the ideal gun theory:[5,6]

$$\tau = \frac{(2M_p c_o)}{[(\gamma + 1)A_p p_o]} , \qquad (1)$$

*The high frequency component of this trace results from the impact of the solenoid valve stem when fully open.

where M_p and A_p are the pellet mass and cross-sectional area, respectively, and γ, p_0, and c_0 are the specific heat ratio initial pressure (measured maximum breech pressure), and initial sound velocity of the propellant, respectively. The solid curves of Fig. 3 are the ideal gun theory muzzle velocities for room temperature helium propellant and for hydrogen propellant at 400 K. These curves are the solutions, u_m, of the following equation:

$$\frac{L}{\tau} = u_{max}\left[\frac{(\gamma - 1)}{2} + \left(1 - \frac{u_m}{u_{max}}\right)^{-(\gamma+1/\gamma-1)} - \frac{(\gamma + 1)}{2}\left(1 - \frac{u_m}{u_{max}}\right)^{-(2/\gamma-1)}\right], \tag{2}$$

where $u_{max} = 2c_0/(\gamma - 1)$ is the propellant escape velocity (maximum attainable velocity). The velocities achieved for helium-driven pellets are 0.8-1.0 times the values predicted by the ideal gun theory, exceeding the propellant initial sound speed, c_0 = 1.0 km/s, for L/τ values greater than 4 km/s. The hydrogen-driven pellet velocities, which include the highest value yet achieved in a pneumatic injector (1.4 km/s at L/τ = 4.9 km/s), fall well below the ideal gun theory predictions. Other inconsistencies between the ideal gun theory and these experimental results are evident in the pressure transients of Fig. 2(c), which were obtained for a 1.4-km/s hydrogen-driven pellet. As in Fig. 2(a), we see that the muzzle pressure maximum, 0.30 MPa, occurs well after the pellet has exited the barrel; this may result in part from the fact that the pellet residence time in the barrel is comparable to or less than the valve opening time. Moreover, the maximum muzzle pressure is only one-third of the value predicted from the ideal gun theory,

$p_{muzzle} = p_{breech}[1 - (\gamma - 1)u_m/2c_o]^{2\gamma/(\gamma-1)} = 0.88$ MPa. These observations have motivated the development of a more complex gas dynamic theory which includes propellant friction, heat exchange, and finite valve opening times.

III. NONIDEAL GAS DYNAMIC THEORY

The schematic diagrams of Fig. 4 show the pellet driver system, geometry and boundary conditions appropriate to the ideal gun and detailed gas dynamic pellet acceleration calculations. In the ideal gun theory treatment[6] the initial boundary conditions are $p(x,0) = p_0$ for $x < 0$, $p(x,0) = 0$ for $x > 0$, $u_{fluid} = 0$ everywhere, and $u_{pellet} = 0$. As the pellet moves a rarefaction wave is launched in the negative x direction into the stagnant propellant. At the pellet surface we require that $u_{pellet} = u_{fluid}$ and calculate the fluid pressure exerted on the pellet from the rarefaction wave characteristic, $dp = \rho c\, du$, where ρ and c are the fluid density and local sound velocity. In the more detailed gas dynamic treatment a valve admits propellant into the driver chamber, which is stepped down at L_D (9.0 cm), over a distance L_Δ (0.84 cm), from diameter D_1 (0.26-cm) to diameter D_2 (0.16-cm). The pellet is positioned initially at the entrance to the barrel, which is under vacuum when the valve is opened (over a typical time interval of several hundred microseconds). The breech pressure is programmed to match the measured pressure transients. When the shear stress in the pellet exceeds the yield strength, the pellet shears free from the forming assembly and is driven by the pressure of the gas.

The Navier-Stokes equations for the fluid driver in an equivalent one-dimensional system are (in conservation-law form):[8,9]

$$\frac{\partial \rho(x,t)}{\partial t} = -\frac{1}{A}\frac{\partial}{\partial x}(mA) ,$$

$$\frac{\partial m(x,t)}{\partial t} = -\frac{1}{A}\frac{\partial}{\partial x}\left[\left(p + \frac{m^2}{\rho}\right)A\right] + \frac{1}{A}\frac{dA}{dx}p - F , \tag{3}$$

$$\frac{\partial e(x,t)}{\partial t} = -\frac{1}{A}\frac{\partial}{\partial x}\left[\frac{m(e + p)A}{\rho}\right] + q ,$$

where

$$p = (\gamma - 1)\, e - \frac{m^2}{2\rho} \text{ is the fluid pressure ,} \tag{4}$$

q = heat source per unit volume,

ρ = mass density,

m = mass flux = ρu,

u = fluid velocity in direction of pellet motion,

e = total (internal plus kinetic) energy per unit volume,

$A(x)$ = cross-sectional area of tube,

and F is the wall friction term defined in terms of the friction factor f as[8]

$$F = \frac{2f\rho}{D} u|u| \tag{5}$$

with D as the tube diameter. The dimensionless coefficient f is empirically found[8] to be $\sim 2 \times 10^{-3}$ for conditions typical of these experiments (Reynolds number $\sim 2 \times 10^5$). The heat transfer, q, is estimated using the Reynolds analogy[8]

$$q = \frac{2f}{D}(\rho u c_p)(T_{wall} - T_{AD}) , \tag{6}$$

where T_{AD} is the adiabatic wall temperature:

$$T_{AD} = T_{gas}\left[1 + R\left(\frac{\gamma - 1}{2}\right)M^2\right] . \tag{7}$$

In Eq. (7) M is the Mach number and R is the recovery factor, taken to be 0.85. As boundary conditions, we specify the pressure and temperature of the plenum to the left of the valve [Fig. 4(b)] and require $u = 0$ to model the thermodynamics of the reservoir. At the right we take $u_{fluid} = u_{pellet}$, as the pellet accelerates. The pellet is modelled as a point mass obeying Newton's equations. The fluid equations are solved as an initial value problem, with an initial small pressure (and density) present in the chamber. The method used is a two-step Eulerian Lax-Wendroff scheme, which is iterated.[10] These computations were performed on the National Magnetic Fusion Computing Center CRAY machines.

The method should produce an accurate treatment of shocks, since the equations are solved in conservative form. The evolution of the entropy is used as a diagnostic check. The equations, with $F = q = 0$, imply that $s(x,t) = c_v \ln(p/\rho^\gamma)$ should be carried with the fluid velocity except for shock discontinuities and the influx of s from the reservoir. The propellant pressure, velocity, entropy, and temperature for a room temperature helium-driven pellet are plotted versus time and position (relative to the chamber inlet) in Figs. 5(a)-(d). A contact discontinuity forms at the chamber entrance as the reservoir valve begins to open [Fig. 5(a)]. Deceleration of the inlet gas [time ~70 μs in Fig. 5(b)], caused by chambrage and pellet inertia, produces $p\Delta V$ work, raising the gas pressure [Fig. 5(a)], and temperature [Fig. 5(d)] at the

chamber/barrel interface. The rapid compression generates a shock wave [Fig. 5(c)] which propogates from the chamber/barrel interface back to the chamber inlet [Fig. 5(a)]. The shock is then reflected as a rarefaction wave (time ~285 μs), which reduces the chamber and barrel pressures as it propagates forward [Fig. 5(a)].

This complex interaction involving an initial pressure surge, compressional heating, shock reflection from the chamber/barrel interface, rarefaction wave reflection from this shock, and the contact discontinuity between the reservoir and chamber propellant results in propellant heating to temperatures exceeding 1000 K [Fig. 5(d)] and pressure oscillations in the chamber and gun barrel [Fig. 5(b)]. These oscillations violate the constant breech pressure assumption of the ideal gun theory and thus destroy the simple L/τ velocity scaling of Eq. (2). For comparison the dashed curves superimposed on Fig. 3 are the nonideal theory pellet velocities for helium and hydrogen. These curves compare reasonably well with the pellet velocity data. They also show interference effects resulting from reflected shocks and rarefaction waves, which may account for the velocity scatter observed in the data of Fig. 4.

IV. CONCLUSIONS

Pellet velocities as high as 1.4 km/s have been attained using high temperature hydrogen propellant. The pneumatic pellet injector performance is adequately modelled by a one-dimensional gas dynamic theory incorporating propellant friction and heat transfer, finite gun geometry, chambrage, and time-dependent boundary conditions. Further theoretical and experimental studies of the effects of propellant auxiliary heating, gun chambrage, barrel temperature and length, etc., on gun performance are planned.

ACKNOWLEDGMENTS

The authors wish to acknowledge the assistance provided by C. E. Thomas and the efforts of F. Bunner in setting up much of the experimental hardware. Research sponsored by the Office of Fusion Energy, U.S. Department of Energy, under contract W-7405-eng-26 with the Union Carbide Corporation.

REFERENCES

[1] S. L. Milora et al., Proc. 9th Int. Conf. on Plasma Physics and Controlled Nuclear Fusion Research, IAEA, Vienna (in press).

[2] S. L. Milora et al., Nucl. Fusion 20, 1491 (1980).

[3] S. L. Milora et al., Bull. Am. Phys. Soc. 25, 927 (1980) and Nucl. Fusion 22 (in press).

[4] K. Buchl and G. Vlases, Bull. Am. Phys. Soc. 26, 888 (1981).

[5]S. L. Milora and C. A. Foster, Rev. Sci. Instrum. 50, 482 (1979).

[6]L. D. Landau and I. M. Lifshitz, *Fluid Mechanics*, Addison-Wesley, Reading, Massachusetts (1959).

[7]C. E. Thomas, Ph.D. dissertation, Massachusetts Institute of Technology (1980).

[8]A. Shapiro, *Compressible Fluid Flow*, Vol. 2, Ronald Press, New York (1959).

[9]R. Richtmeyer and K. Morton, *Difference Methods for Initial Value Problems*, Wiley Interscience, New York (1967).

[10]S. Abarbanel and G. Zwas, Math. of Comput., 549 (1969).

FIGURE CAPTIONS

FIG. 1. Modified pellet line with guide tube and diagnostics.

FIG. 2. Signal traces and shadowgraphs (a)-(b) for a 1-km/s helium-driven pellet and (c)-(d) for a 1.4-km/s hydrogen-accelerated pellet.

FIG. 3. Pellet velocity vs L/τ for 295 K helium (Δ) and 400 K hydrogen ($\square$) propellants. The solid curves are the ideal gun theory calculations for these two cases. The broken curves are the corresponding nonideal gas dynamic calculations.

FIG. 4. Injector models used in (a) the ideal gun and (b) the detailed gas dynamic calculations.

FIG. 5. Propellant (a) pressure, (b) velocity, (c) entropy, and (d) temperature vs position and time (helium propellant initially at room temperature). In these plots position is normalized to the total chamber plus barrel length L_T [see Fig. 4(b)].

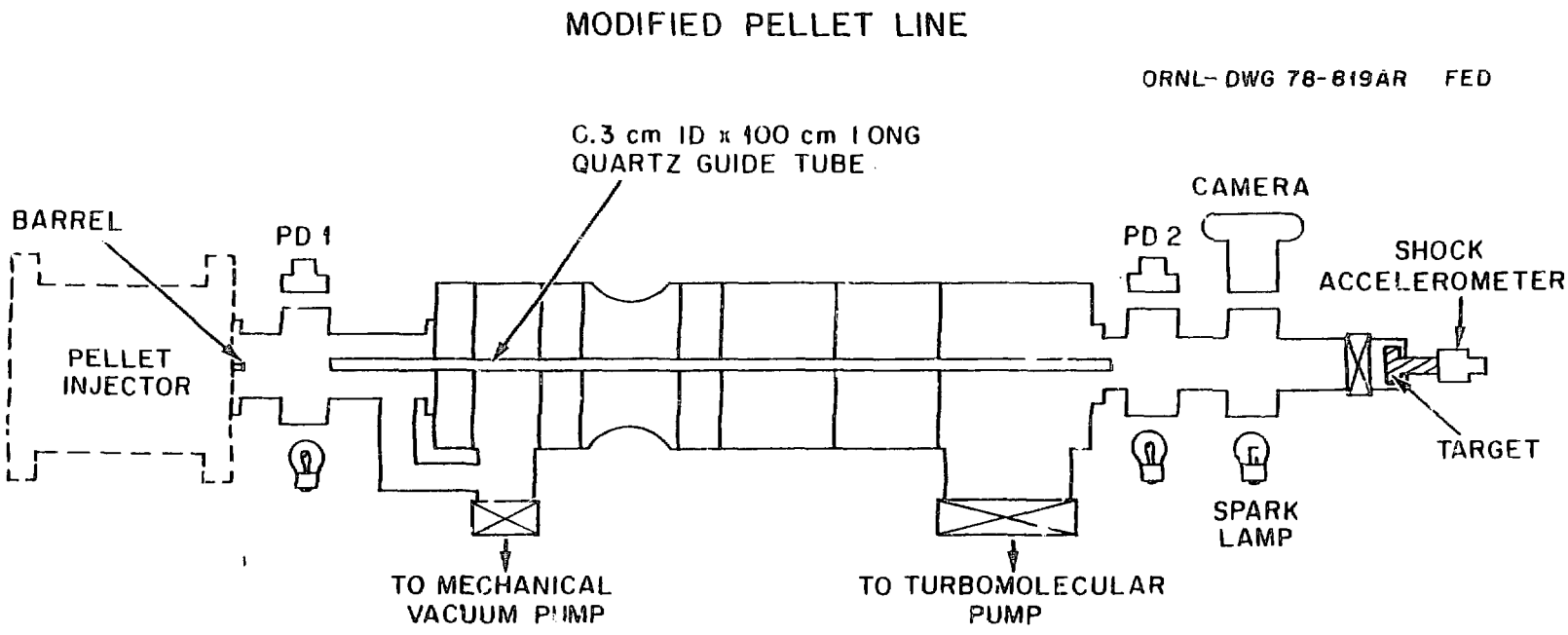
MODIFIED PELLET LINE
ORNL-DWG 78-819AR FED
0.3 cm ID x 100 cm LONG
QUARTZ GUIDE TUBE
CAMERA
BARREL
PD 1
PD 2
SHOCK
ACCELEROMETER
PELLET
INJECTOR
TARGET
SPARK
LAMP
TO MECHANICAL
VACUUM PUMP
TO TURBOMOLECULAR
PUMP

Fig. 1

SIGNAL TRACES AND SHADOW GRAPHS

ORNL-PHOTO 4000-82 FED

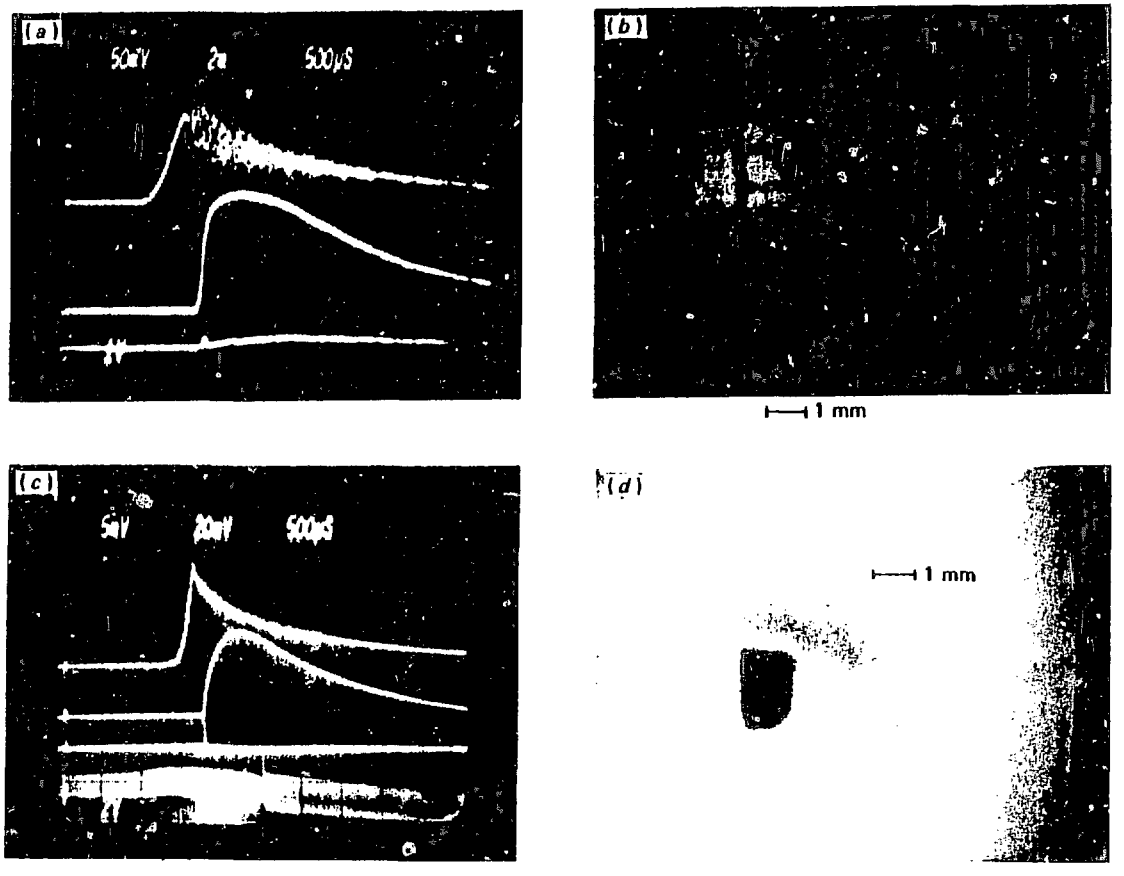

P_{BREECH} = 2.34 MPa

P_{MUZZLE} = 0.14 MPa

PD1

P_{BREECH} = 5.84 MPa

P_{MUZZLE} = 0.30 MPa

PD1

PD2

Fig. 2

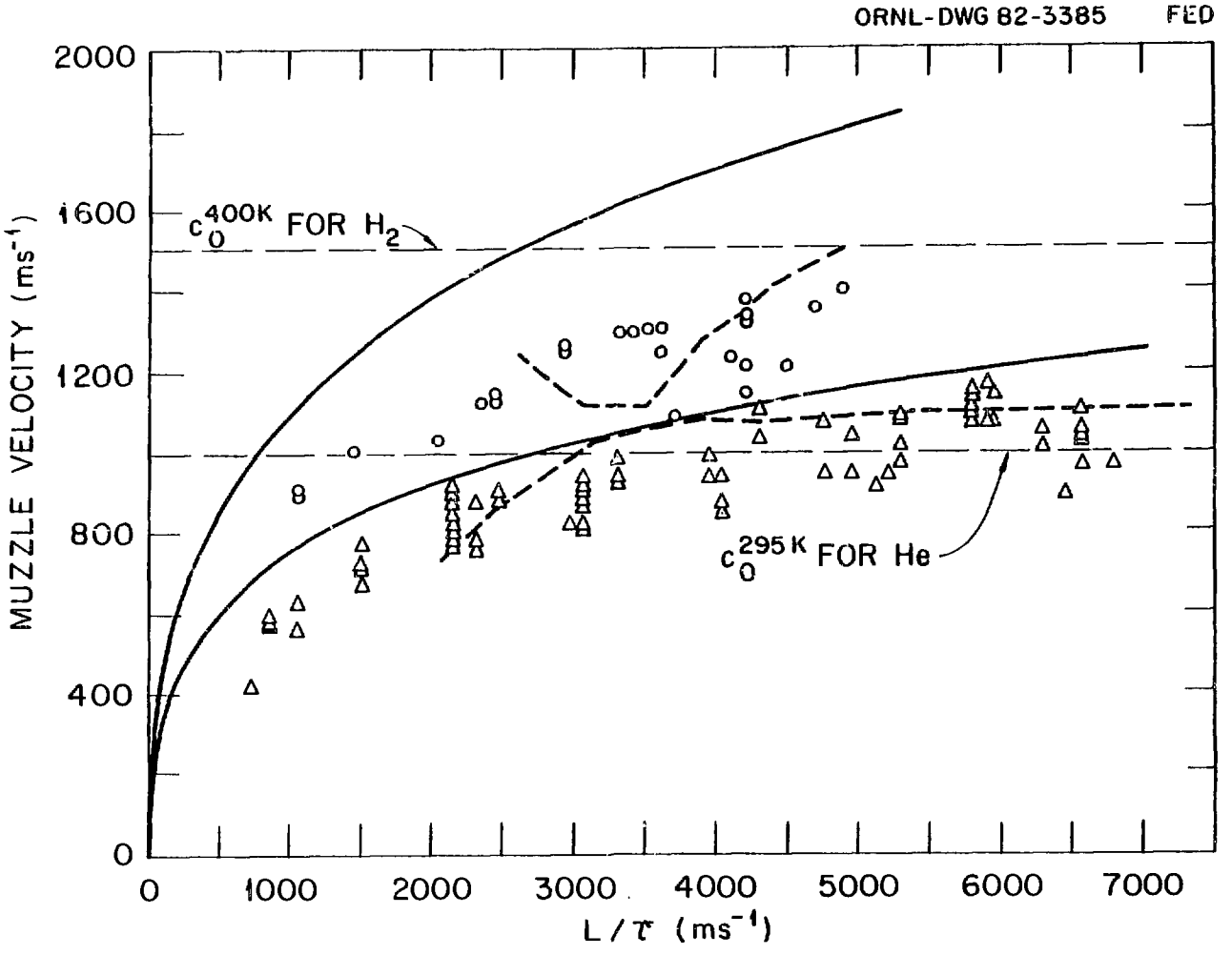
ORNL-DWG 82-3385 FED
MUZZLE VELOCITY (ms⁻¹)
2000
1600
1200
800
400
0
c_0^{400K} FOR H_2
c_0^{295K} FOR He
0
1000
2000
3000
4000
5000
6000
7000
L / τ (ms⁻¹)

Fig. 3

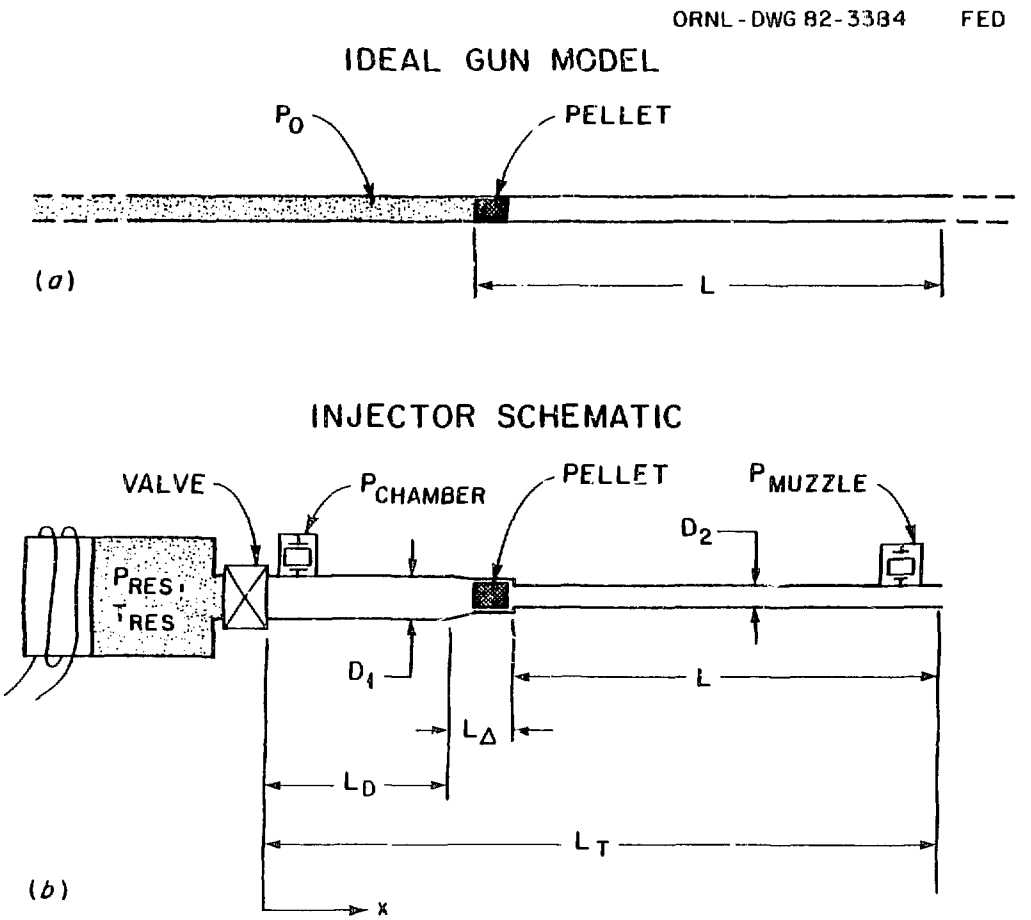
ORNL - DWG 82-3384 FED
IDEAL GUN MODEL
P_0
PELLET
(a)
L
INJECTOR SCHEMATIC
VALVE
$P_{CHAMBER}$
PELLET
P_{MUZZLE}
D_2
P_{RES}
T_{RES}
D_1
L
L_Δ
L_D
L_T
(b)
x

Fig. 4

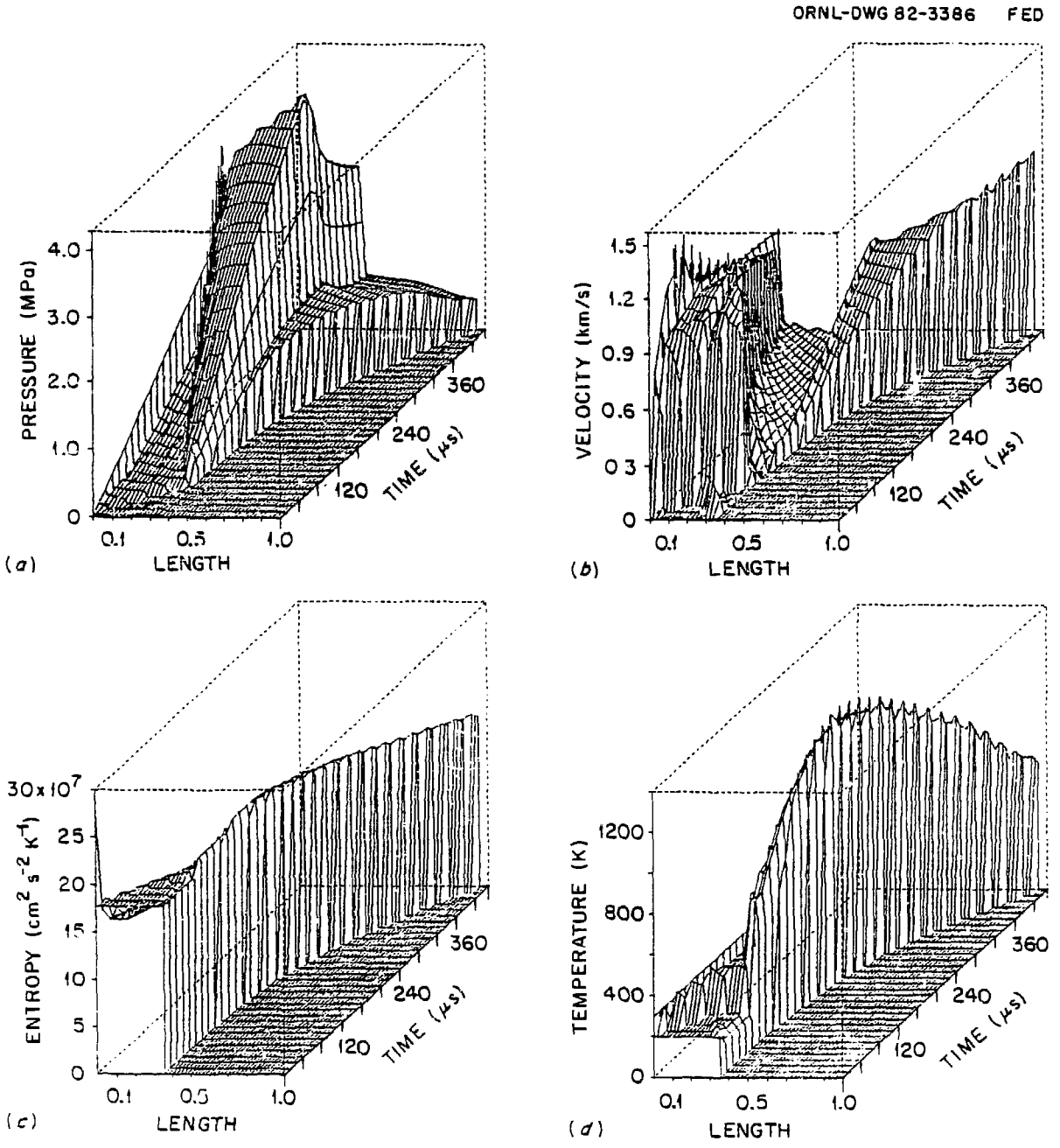
ORNL-DWG 82-3386 FED
PRESSURE (MPa)
4.0
3.0
2.0
1.0
0
0.1
0.5
1.0
LENGTH
120
240
360
TIME (μs)
(a)
VELOCITY (km/s)
1.5
1.2
0.9
0.6
0 3
0
(b)
ENTROPY (cm² s⁻² K⁻¹)
30x10⁷
25
20
15
10
5
0
(c)
TEMPERATURE (K)
1200
800
400
0
(d)

Fig. 5